JOURNAL OF MATERIALS SCIENCE 32 (1997) 6163–6173

Ceramic coatings by ion irradiation of polycarbosilanes and polysiloxanes

Part I *Conversion mechanism*

J. C. PIVIN*
Centre de Spectrométrie Nucléaire et de Spectrométrie de Masse, Bâtiment 108, 91405 Orsay Campus, France

P. COLOMBO
Università di Padova, Dipartimento di Ingegneria Meccanica-Settore Materiali, via Marzolo 9, 35131 Padova, Italy

Changes of composition and structure of various types of polysiloxanes and polycarbosilanes when submitted to irradiation with ions of increasing mass, were analysed by means of several ion-beam analytical techniques, Raman and Fourier transform–infrared spectroscopies. Ion irradiations is as efficient as annealing at temperatures above 1000 °C for releasing hydrogen from these organic–inorganic polymers, and the radiolytic evolution of hydrogen is selective, whereas methane, silanes and carbon monoxide are also evolved during heat treatments. The kinetics of the polymer conversion into amorphous ceramics depends strongly on the linear density of energy transferred by ions to electron shells of target atoms, according to the ion energy per nucleon and to the nature of the side groups. Some of the carbon atoms segregate in clusters exhibiting a diamond-like hybridization state, in contrast to the clusters of turbostratic graphite formed in pyrolysed films.

1. Introduction

A wide assortment of ceramic coatings with useful heat-, corrosion- and wear-resistance or optoelectronic properties are currently produced by means of chemical and physical vapour deposition (CVD, PVD), sputtering and plasma spraying. The pyrolitic conversion of alkoxide gels or organometallic polymers (also referred to as organic–inorganic because their backbone is not constituted by carbonaceous moities) is a priori a more versatile and economical route. Indeed, the precursors can be homogeneously deposited form a solution on irregular surfaces such as fibres, and composite films can be obtained simply by mixing solutions [1]. The synthesis of carbide or nitride films (SiC, SiOC, TiC, TiN, BN) by polymer pyrolysis has been less explored [2–5], probably because a strict control of the processing atmosphere is crucial for avoiding the release of boron, carbon or nitrogen and the formation of oxide films [6–8]. In fact, treatments at temperatures of the order of 1200 °C are necessary for evolving most of the hydrogen from carbide and oxycarbide precursors, due to the high stability of single C–H bonds and to the formation of an oxide casing around carbide particles.

Recently, it has demonstrated that ion irradiation is an alternative method which offers the advantage over such high-temperature treatments of producing a more preferential and nearly as complete release of hydrogen [9–10]. The higher efficiency of ion-induced ionizations in breaking and cross-linking bonds in organic polymers, than those of other radiations and thermochemical reactions, is well established [11].

The study of the conversion process by ion irradiation was extended in this paper to polymeric and alkoxide precursors with different C/Si and O/Si ratios. It was particularly interesting to investigate the influence of the nature of carbonaceous side groups and of the mass and energy of ions on the rates of conversion and structural transformations, because in the case of organic polymers the respective yields of chain cross-linking and scission depend critically on the densities of ionizations and atomic displacements, according to the energy per nucleon of ions [11, 12]. Measurements of the film hardness, a property highly sensitive to the conversion of polymers into ceramics and of primary interest for coatings, are reported in a second paper (Part II [13]), as also the modifications of film properties produced by further heat treatment of irradiated specimens.

* Author to whom correspondence should be addressed.

0022–2461

2. Experimental procedure

2.1. Film preparation

Two different precursors for SiC films were used: polycarbosilane (PCS, Dow Corning X9-6348), and allylhydridopolycarbosilane (AHPCS, Starfire Systems Inc., Watervliet, NY). Both were dissolved in HPLC hexane.

SiOC films were produced from ethanolic solutions of two different preceramic polymers: methylhydroxylsiloxane and phenylmethylhydroxylsiloxane (SR350 and SR355, General Electric Silicone Products Div., Waterford, NY), and of an alkoxide: phenyltriethoxysilane $C_6H_5Si(OC_2H_5)_3$ (PTES, Aldrich Chimica, Milan). Water in the molar ratio $H_2O/PTES = 3$ and 1 N HCl in the molar ratio $HCl/PTES = 0.01$ were added to the alkoxide solution. The hydrolysis of ethoxy groups of the PTES alkoxide yields $C_6H_5Si(OH)_3$ molecules which then condense into a siloxane three-dimensional gel.

Fig. 1 shows the chemical structures of the precursors used in this work. One has to bear in mind that they represent only a simplification of the actual polymer structure, that usually involves the presence of branching and rings [14–17].

The dilution of the various solutions was adjusted in order to obtain films with thicknesses in the range 600–1000 nm, optimal for irradiation and analyses. The solutions were spun at 3000 r.p.m. on $\langle 100 \rangle$ silicon wafers in a glove box with a controlled relative humidity of about 20%. Wafers were ultrasonically cleaned using a diluted HF solution and acetone. Part of the specimens were heat treated at a temperature of 1000 °C for 1 h in vacuum (10^{-6} torr; 1 torr = 133.322 Pa). Note that annealed films generally exhibited some cracks and AHPCS films systematically flacked off the substrate, while irradiated ones (including AHPCS) were defect-free.

2.2. Irradiation treatments and simulations

Pieces were cut from the same wafer for performing a series of irradiations with incremental ion doses, Φ, ranging from 1×10^{13}–5×10^{16} cm^{-2}. The films were irradiated at room temperature with 200 keV He, 500 keV C or 3 MeV Au ions, delivered by the ARAMIS accelerator of CSNSM [18]. The ion power was limited to 0.1 W cm^{-2} in order to avoid a significant heating of the samples. Ion species and energies were selected for their large difference of stopping cross-sections, S_e and S_n, by electrons and nuclei, and for penetrating at larger depth than the film thicknesses, without regard to their chemical nature. The transformation rates for these particular conditions of irradiation were also well determined in several organic polymers [11] and in polyphosphazene films [19].

Simulations of collision cascades were performed, using the TRIM code [20, 21], for each polymer with their as-deposited composition and also for films completely depleted in hydrogen (using the measured densities in both cases for depth scales). Indeed, the variation of the linear densities of energy transferred

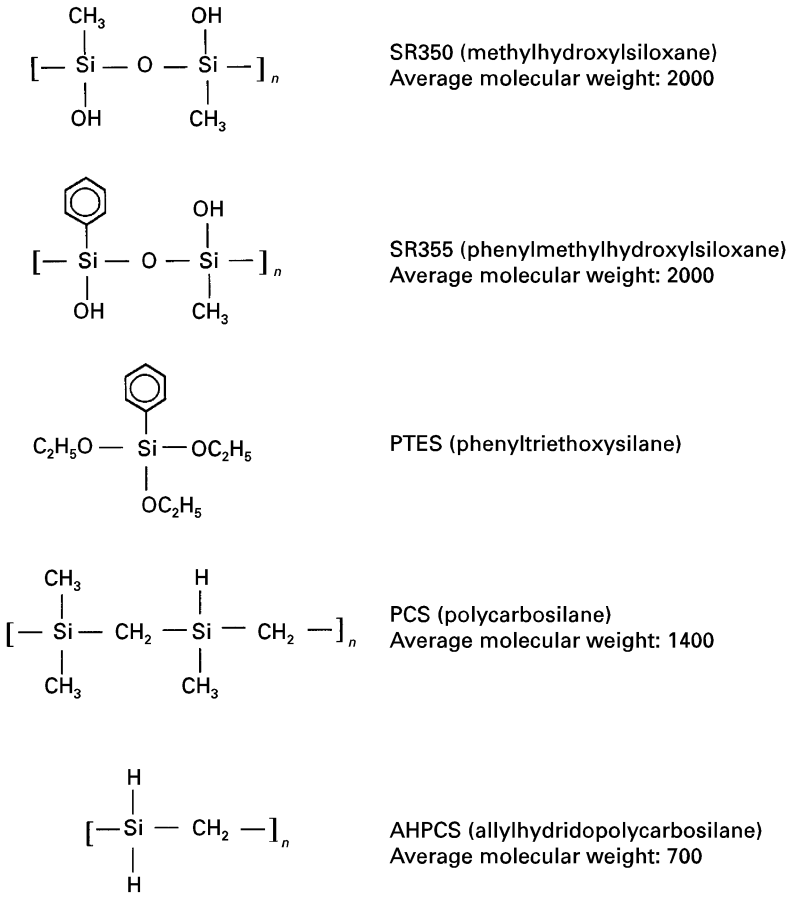

Figure 1 Chemical structure of precursors used for preparing SiC and SiOC thin films.

to electrons, S_e, and nuclei, S_n (also termed stopping powers) as a function of the progressive dehydrogenation of polymers must be at least estimated, if not taken into account, when analysing the changes of properties versus the amount of deposited energy $S_e \times \Phi$ or $S_n \times \Phi$. The values of stopping powers reported in Table I were averaged over the same depth range, of 500 nm, as other parameters (compaction, composition, hardness) hereafter. If gradients of these parameters were sometimes observed at larger depths, they were disregarded because of the more important contribution of displacements to their modification at depths close to the ion ranges (1–1.5 μm) and to the displacement-induced mixing with the substrate. Note that S_e values reported in Table I include the contribution of recoils, noticeable only in the case of 3 MeV Au irradiation.

When comparing materials irradiated with a given ion species, S_e and S_n values increase roughly as the mean mass of target atoms. They vary the most with the dehydrogenation in the case of gold irradiation. Because the ion doses, Φ, and the corresponding amounts of energy, $S_e \times \Phi$, were varied by several orders of magnitude, it was justified in plotting the kinetics of compaction and hydrogen evolution (and hardness in Part II [13]) versus eneregy, to use the same S_e value for all polymers irradiated with a given ion species, equal to the mean S_e in dehydrogenated films. Stronger variations in hydrogenated films were initially disregarded when analysing the kinetics.

2.3. Compositional and microstructural analysis

Several ion-beam analysis techniques were used for determining the film compositions. Experiments of Rutherford back-scattering spectrometry (RBS) and elastic recoil detection analysis (ERDA) were performed with the ARAMIS accelerator. The AGLAE accelerator, at the Laboratoire des Musées de France, Paris, was used for performing complementary nuclear reaction analysis (NRA). The yields of protons produced by $^{12}C(d, p_0)^{13}C$ reactions and by $^{16}O(d, p_1)^{17}O$ reactions were measured at a collection angle of 150° with respect to the incident beam, of energy 950 keV for carbon analysis and of 900 keV for oxygen analysis. These yields provided directly the areal densities of carbon and oxygen (number of atoms per unit area) from which were deduced the stoichiometries Si_1–C_x–O_y of the films, assuming that the areal density of silicon atoms did not decrease due to their sputtering during irradiation, to microscopic spallings or to the volatilization of SiO during annealing (generally observed at temperatures above 1200 °C [22]). Depth profiles of the concentration, z, of hydrogen atoms per monomer unit $Si_1C_xO_y$ were determined by means of ERDA analysis with an incident beam of 3 MeV He. As usual, spectra were recorded with a glancing angle of 15° with respect to the surface for both the incoming helium and outgoing hydrogen beams. RBS spectra with helium ions of 1.5 MeV, or non-Rutherford back-scattering spectra with hydrogen ions of 1.6 MeV (giving higher signals for carbon, oxygen atoms), were recorded for cross-checking the Si_1–C_x–O_y–H_z stoichiometries, the total density of atoms per unit area, and more especially that of silicon. Note that the helium doses used for recording ERDA spectra of pristine or slightly irradiated specimens was limited to 1 μC, in order to avoid production of a significant radiolysis with respect to the smallest dose of 200 keV He ions. Spectra recorded with incremented helium doses in the range 0.1–2 μC showed that no hydrogen radiolysis occurred during the course of these ERDA experiments.

Measurements of film thicknesses, t, were performed using a tactile profilometer (DEKTAK 3030ST Instruments) and allowed to derive: (i) bulk densities of atoms in combination with the areal densities measured by ion beam analysis; (ii) compaction values $\Delta t = (t_0 – t/t_0)$, where t_0 is the initial thickness. The uncertainty in Δt estimations was of 3%, due to fluctuations of the initial thickness of the order of 10 nm (amplitude of striations in the spin coatings).

Changes in the chemical structure of the coatings were assessed by infrared (Fourier transform–infrared, FT–IR) and Raman spectroscopies. The FT–IR spectra were recorded in transmission from 4000–400 cm^{-1} at 1 cm^{-1} resolution, using a Perkin–Elmer System 2000 spectrometer. The Raman spectra were collected using a DILOR X–Y microspectrometer fitted with a multichannel CCD detector, and the bandpass was 2 cm^{-1}. The excitation source was the 514.5 nm line of a Spectraphysics 2017 argon-ion laser, operated at 2 mW, and the beam was rastered over 75 μm, in order to avoid heating of the films.

TABLE I Linear densities of energy transfer, S_e, to electrons and, S_n, to nuclei (eV $cm^2/10^{15}$ ions × atoms; simplified by eV in text), calculated by means of the TRIM code for 1.0 μm thick films hydrogenated (Y) or not (N). S_e and S_n values are averaged over a range of depths of 500 nm and their gradients are indicated by margins of error. Values of S_e used in Figs 3–5 are 29 eV (He), 75 eV (C), 420 eV (Au).

Ions and energy	Hydrogen	SR350		SR355		PTES		PCS		AHPCS	
		Se	Sn	Se	Sn	Se	Sn	Se	Sn	Se	Sn
200 keV He	Y	25 ± 2.5	0.2	27 ± 4	0.2	22 ± 2	0.1	20 ± 2.5	0.1		
	N	32 ± 7	0.3	27 ± 4	0.2	29 ± 5	0.3	34 ± 9	0.3		
500 keV C	Y	64 ± 8	1.7	68 ± 11	1.6	53 ± 7	1.5	57 ± 7	2.5		
	N	78 ± 16	2.8	74 ± 15	2.4	73 ± 14	2.5	84 ± 20	2.4		
3 MeV Au	Y	355 ± 40	230 ± 35	335 ± 30	210 ± 30	290 ± 25	180 ± 10	280 ± 20	155 ± 35	255 ± 30	150 ± 15
	N	440 ± 80	360 ± 50	420 ± 50	315 ± 50	410 ± 40	280 ± 30	450 ± 80	350 ± 40	470 ± 90	365 ± 40

3. Results

3.1. Changes of composition, thickness and density

Unfortunately, it is not possible with most accelerators to perform ERDA analyses *in situ* (unlike RBS ones) because of the particular geometry of these experiments. Indeed, polymers tend to oxidize and hydrolyse when exposed to the ambient after irradiation, if all free radicals formed under the effect of ionizations are not cross-linked into some three-dimensional network [11]. Oxygen and water also penetrated throughout the presently studied films when uncompletely cross-linked (slightly irradiated), and the contribution of the post-irradiation hydrogen intake to the measured hydrogen content could not be subtracted for estimating the hydrogen loss during the irradiation itself. In some cases, such as for the SR350 film irradiated with 10^{16} He (the ERDA spectrum of which is shown in Fig. 2), the hydrolysis was more superficial and the ERDA profile of scattered hydrogen atoms exhibited a peak near the surface (on the high-energy side). This peak was not included when analysing variations of hydrogen content with the ion fluence or species. Other examples of profiles displayed in Fig. 2 give evidence of the homogeneity of the hydrogen evolution throughout the film thickness.

The degree of oxidation as a funtion of the film and ion natures and of the dose could be estimated on the basis of NRA measurements. In all cases, including polycarbosilane films containing oxygen only as impurity, the areal density $N(\mathrm{O})$ of oxygen atoms could be normalized to a constant density $N(\mathrm{Si_0})$ of silicon for a given series of irradiation of the same pristine film, for obtaining an Oxygen stoichiometry $y = (N(\mathrm{O})/N(\mathrm{Si_0})$ independent of film thickness. Indeed RBS profiles were perfectly fitted with the sum of (N(O), N(C), N(H) determined by NRA and ERDA and of the initial density $N(\mathrm{Si_0})$. The stoichiometry y in PCS increases from 0.10 in the pristine polymer to 1.0 in specimens irradiated with helium and remains at this high level for doses in the range 2.5×10^{15}–5×10^{16} (S_e = 70–1500 eV). It increases only up to 0.60 in PCS irradiated with 2.5×10^{14} or 5×10^{13} Au, then decreases quickly to 0.06. In the case of polysiloxanes, the oxygen content could be normalized as well to $N(\mathrm{Si_0})$ or to $N(\mathrm{O_0})$, for calculating a relative increase of oxygen concentration: $\Delta\mathrm{O} = [N(\mathrm{O})–N(\mathrm{O_0})]/N(\mathrm{O_0})$. Variations of ΔO plotted in Fig. 3 show that it augments more in phenyl-containing polysiloxanes than in SR350. ΔO reaches a maximum for $S_e\times\Phi$ values in the range of 20–50 eV then tends back to zero, whatever the ion species. Note that no significant changes of N(C) are observed during irradiation of the presently studied polymers: fluctuations of no more than 3% correspond to thickness variations.

The relative decrease of hydrogen concentration in the homogeneous part of films, $\Delta\mathrm{H} = (z_0 - z)/z_0$, directly given by the fits of ERDA profiles, is also equal to $[N(\mathrm{H_0}) - N(\mathrm{H})]/N(\mathrm{H_0})$ because N(Si) is constant. As already stated, it cannot be corrected for the post-irradiation hydrolysis because the film reacts also with oxygen and it is not certain that one OH^- and one H^+ are fixed for each water molecule penetrating into the polymer. On the other hand, mean z_0 values given in Tables II and III were used in calculations of ΔH but they varied by ± 10% in films of the same type. In other respects, y_0 and z_0 measured in SR350 and SR355 films correspond to the compositions of monomers cross-linked through the hydroxide group, $\mathrm{Si(O)_{3/2}(CH_3)}$ and $\mathrm{Si(O)_{3/2}(CH_3)–Si(O)_{3/2}(C_6H_5)}$, respectively (factors $\frac{1}{2}$ indicate that oxygen atoms are shared with a

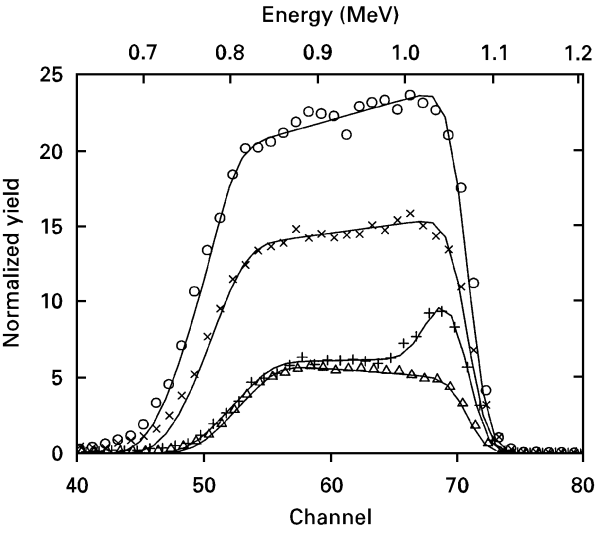

Figure 2 ERDA spectra recorded on SR350 films irradiated with 200 keV He ions at various fluences: (○) 5×10^{14}, (×) 2.5×10^{15}, (+) 1×10^{16}, (△) 5×10^{16} cm^{-2}. (–) Fits with respective H/Si ratios equal to 1.52, 0.94, 0.36, 0.29 in the homogeneous part of the films, of thicknesses 3500, 3200, 2000, 2400×10^{15} atoms cm^{-2}, an outer layer of 550×10^{15} atoms cm^{-2} containing 0.62 H/Si in film (+), and linear gradients from the film content to 0 extending over 500×10^{15} atoms cm^{-2}, at the polymer–silicon interface.

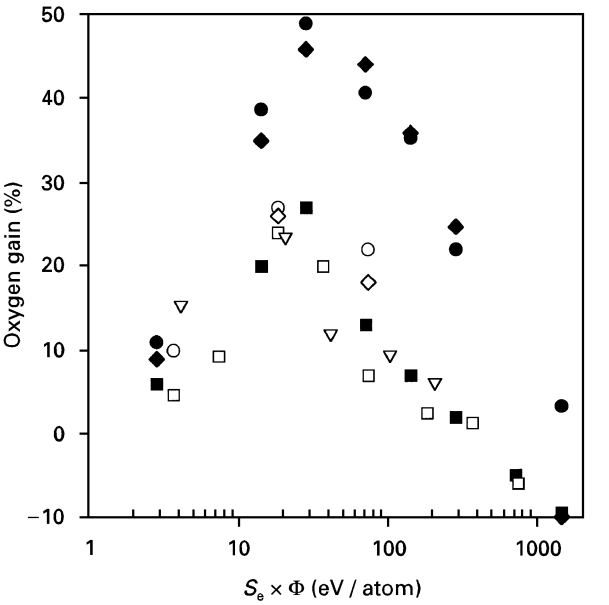

Figure 3 Variations of ΔO with $S_e\times\Phi$ in polysiloxanes: (●) SR355 + He, (■) SR350 + He, (◆) PTES + He, (○) SR355 + C, (□) SR350 + C, (◇) PTES + C, (△) SR355 + Au, (▽) SR350 + Au, (⬢) PTES + Au.

neighbour silicon). On the contrary, those measured in PTES films indicate that only a small part of the OH^- have reacted together. The compositions x_0 and z_0 found for the polycarbosilanes are in agreement with chemical analyses by means of other spectrometric methods [22] and account for the release of three hydrogen atoms initially bound to one silicon atom and two out of three methyls in each monomer of PCS, and for that of 1.3 hydrogens bound to silicon on average in AHPCS.

Variations of ΔH and of the compaction, Δt, versus $S_e \times \Phi$ are reported in Figs 4–6. Both parameters Δt and ΔH vary nearly in proportion to the logarithm of $S_e \times \Phi$ within a given energy range, then they level off. When comparing the kinetics in polysiloxanes, those of PTES and SR355 irradiated with helium ions are strongly different from the others. They are delayed up to 2 eV (ΔH) or 10 eV (Δt) in correlation with the stronger oxidation of these films (Fig. 3). Beside that, the yield of hydrogen radiolytic evolution in PTES irradiated with carbon or gold is also slightly delayed with respect to that in other polysiloxanes. The saturation of the irradiation effect is clearly observed for the three materials when irradiated with gold (because it occurs at smaller $S_e \times \Phi$), and the levels of Δt, ΔH reached are a little lower. The kinetics of compaction and hydrogen evolution in polycarbosilanes depend more on the mass of ions (Fig. 4b and 5b) than in polysiloxanes. If comparing the two types of polymer, the yields are a little higher as is also the rate of compaction in polycarbosilanes (Fig. 6). The compaction of polysiloxanes varies in proportion to the yield of hydrogen evolution, with a slope equal to $\frac{1}{2}$, and all data are along a same line (Fig. 7a). Contrary to that of polysiloxanes, the compaction of polycarbosilanes is proportional to the square of ΔH, with the same rate for all ion species (Fig. 7b), in agreement with the difference in the rate observed in Fig. 6.

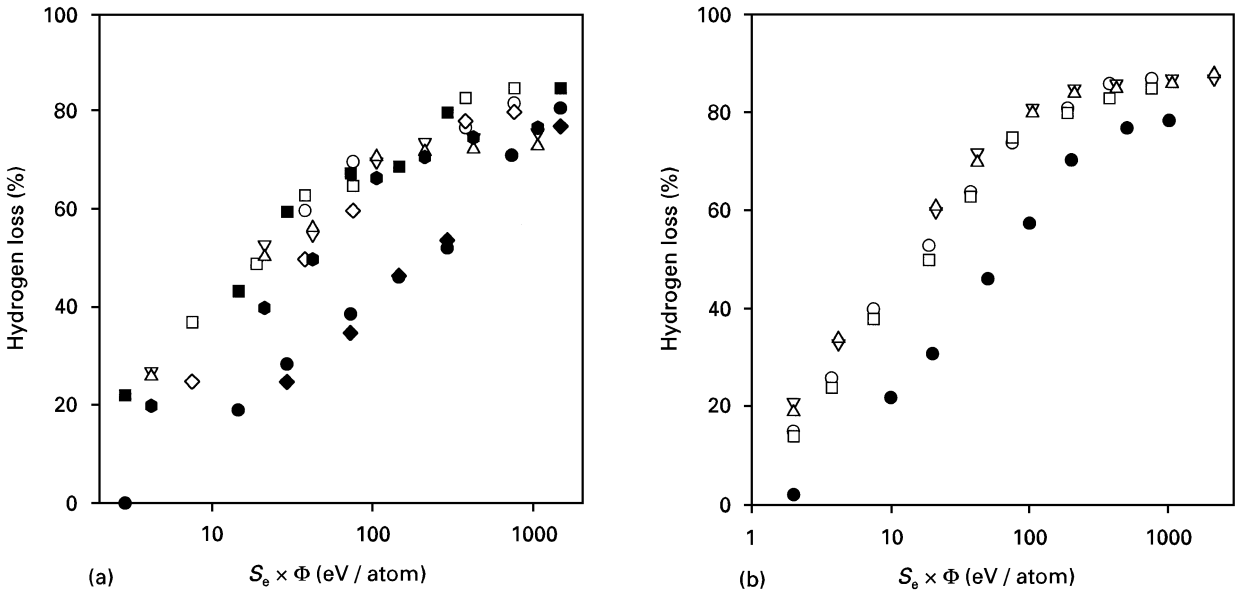

Figure 4 (a) Variations of ΔH with $S_e \times \Phi$ in polysiloxanes (for key, see Fig. 3). (b) Variations of ΔH with $S_e \times \Phi$ in polycarbosilanes: (○) PCS + C, (□) AHPCS + C, (▽) PCS + Au, (△) AHPCS + Au, (●) PCS + He.

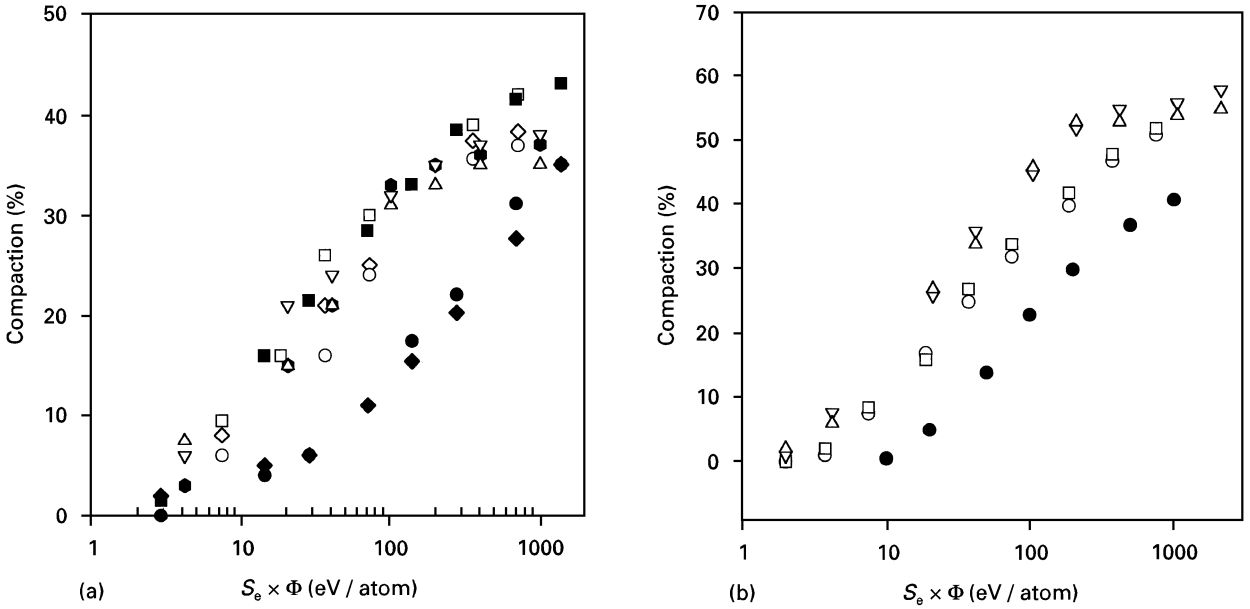

Figure 5 Variations of Δt with $S_e \times \Phi$ in (a) polysiloxanes (for key, see Fig. 3) and (b) polycarbosilanes (for key, see Fig. 4b).

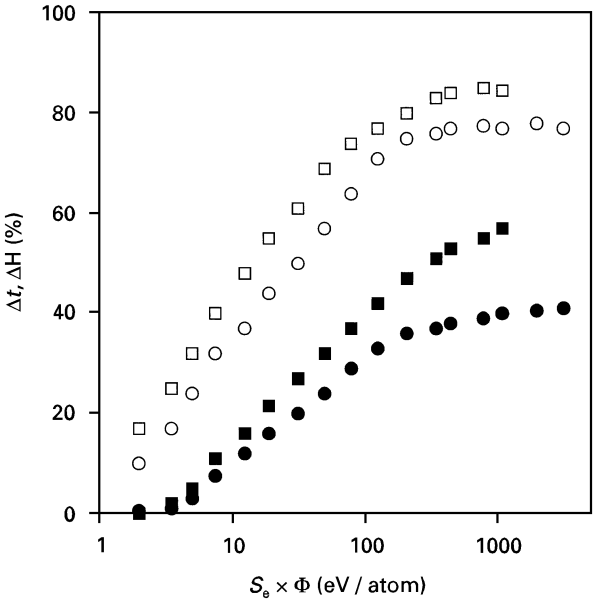

Figure 6 Comparison of (■, ●) the compaction and (□, ○) H loss in (■, □) polycarbosilanes and (●, ○) polysiloxanes. The data relative to the three polysiloxanes or to the two polycarbosilanes for the same $S_e \times \Phi$ are averaged, and the same symbol is used for carbon and gold irradiations. Data relative to helium irradiation are not plotted because of the strong effect of hydrolysis in SR355, PTES and PCS.

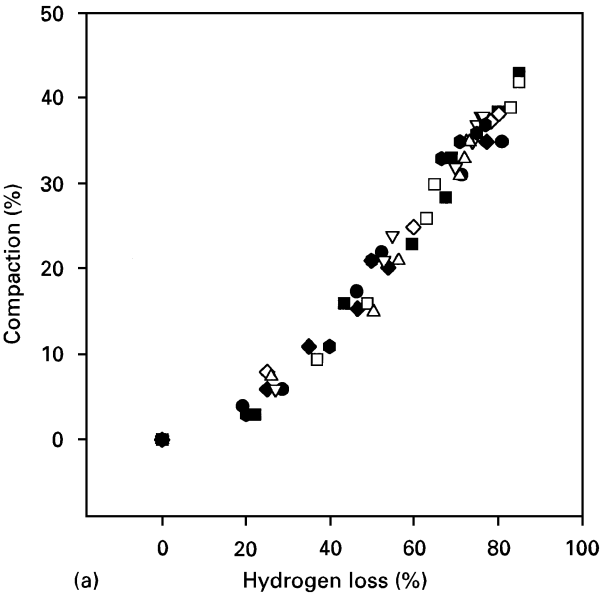

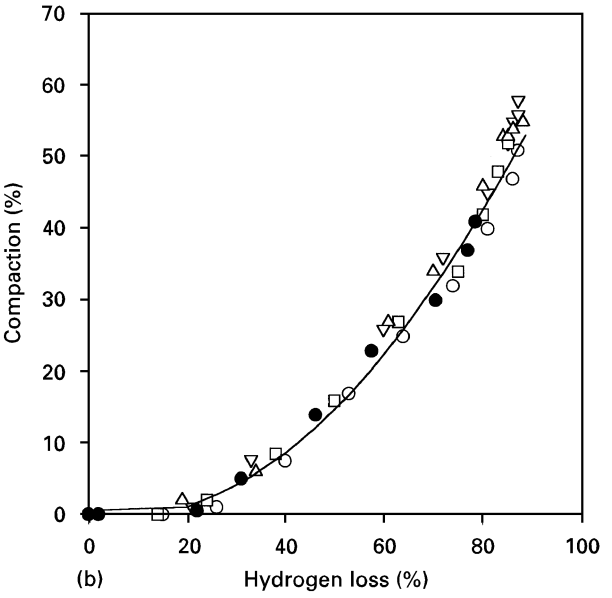

Figure 7 (a) Variations of Δt versus ΔH in polysiloxanes compaction (for key, see Fig. 3). (b) Variations of Δt versus ΔH in polycarbosilanes (for key, see Fig. 4b), and fit with a quadratic law (—).

From areal densities of atoms and thicknesses, the densities of atoms per unit volume, d_{at}, and mass per unit volume, d_w, were derived (the latter being density according to the strictest definition of the term). They were not plotted as a function of the transferred energy because both depend too intrinsically on the changes of oxygen and hydrogen concentrations. Despite its higher significance for solid-state physicists, d_{at} is not a relevant criterion of the conversion in the present case. Indeed, it generally shows a maximum at intermediate ion fluences because $N(O)$ increases while $N(H)$ decreases, so that strongly hydrolysed films would appear more converted than films having lost more hydrogen and any molecular structure at higher ion fluences. Values of densities measured at the ultimate stage of conversion by irradiations and by annealing for 1 h at 1000 °C, are summarized in Tables II and III, together with the film stoichiometries. While no loss of carbon is observed during irradiation, a noticeable loss occurs during annealing in all polymers, depending more on the proportion of carbonaceous groups in the monomer than on the C/Si ratio: 40%–45% of the carbon atoms in SR350, SR355 and PTES, 60% in PCS are lost. Mass spectrograms of gaseous species evolved during the pyrolysis of PCS [22] showed that of methylsilane above 600 °C, then lighter species CH_4, C_2H_6, CO between 800 and 1100 °C. As a consequence of this evolution, unpaired silicon atoms tend to trap oxygen from the residual atmosphere. But the areal amount of oxygen atoms and often the stoichiometry, y, decrease in annealed polysiloxanes because some oxygen is released as CO (and SiO above 1400 °C) and part of the films flake off. However that may be, taking as a reference the density of bulk β-SiC (3.22 g cm^{-3}), the relative densities of irradiated PCS films regardless of the ion nature reach only 65% ± 2%, while that of annealed PCS films is 79% ± 12%, mainly because they contain less carbon. Note that the density of annealed films is estimated with a poor accuracy because only films with thicknesses lower than 700 nm can be annealed without spalling, and their residual thickness of ~170 nm varies locally by 20 nm. Nevertheless, values of 75% were also reported for amorphous PCS-derived fibres annealed under a high argon pressure at 1000 °C (with a reported composition $Si_1C_{1.4}O_{0.4}H_{0.4}$ which is quite different from that of our films $Si_1C_{0.8}O_{0.2}H_{0.2}$) and of 78% for crystalline fibres annealed at 1200 °C [15]. With respect to the density of 2.35 g cm^{-3} of bulk SiOC glass obtained by heat treating the SR350 resin in inert gas at 1300 °C [16, 17], ion irradiations afford to films of this polymer, relative densities of 89% ± 3% as against 88%

TABLES II and III Stoichiometries and densities measured for films subjected to the highest irradiation doses and for annealed films.

TABLE II Polysiloxanes

Film	Treatment	Composition $Si_1C_xO_yH_z$			Density	
		x	y	z	d_w ($g\,cm^{-3}$)	d_{at} (10^{22} at cm^{-3})
SR350	Pristine	1.00 ± 0.05	1.55 ± 0.05	2.9 ± 0.1	1.25	7.5
	He	1.00	1.40	0.29	2.05	7.2
	C	1.00	1.50	0.37	2.16	8.0
	Au	1.00	1.50	0.55	2.06	8.2
	Annealed	0.60	1.28	0.52	2.08	7.5
SR355	Pristine	3.50 ± 0.1	1.50 ± 0.05	4.25 ± 0.25	1.18	7.5
	He	3.55	1.50	1.20	1.72	7.4
	C	3.50	1.50	0.95	1.76	7.8
	Au	3.50	1.50	1.15	1.78	8.1
	Annealed	1.80	1.38	0.40	1.68	6.4
PTES	Pristine	6.00 ± 0.1	1.65 ± 0.1	6.05 ± 0.10	1.22	8.1
	He	6.00	1.55	1.35	1.76	8.4
	C	6.00	1.50	1.19	1.80	8.2
	Au	6.00	1.50	1.50	1.69	8.3
	Annealed	3.50	1.80	1.55	n.m.[a]	n.m.[a]

[a] n.m. = not measured.

TABLE III Polycarbosilanes

Film	Treatment	Composition $Si_1C_xO_yH_z$			Density	
		x	y	z	d_w ($g\,cm^{-3}$)	d_{at} (10^{22} at cm^{-3})
PCS	Pristine	1.90 ± 0.1	0.08 ± 0.02	4.50 ± 0.2	1.10	8.4
	He	1.90	0.92	1.00	2.14	9.0
	C	1.85	0.06	0.60	2.15	8.7
	Au	1.75	0.06	0.62	2.01	8.3
	Annealed	0.80	0.20	0.25	2.45 ± 0.30	7.9 ± 0.94
AHPCS	Pristine	1.00 ± 0.05	0.10	2.70	1.16	7.7
	C	1.00	0.10	0.64	2.25	8.8
	Au	1.00	0.07	0.46	n.m.[a]	n.m.[a]

[a] n.m. = not measured.

for films annealed 1 h at 1000 °C. The densities of SR355 and PTES films completely converted by irradiation are lower by 14%. Larger differences could not be expected between the three polysiloxanes, on account of the very comparable densities of silica and graphite or amorphous carbon (2.20 and 2.30 $g\,cm^{-3}$).

3.2. Structural transformations

Fig. 8 shows FT–IR spectra of PCS and SR350 films submitted to irradiation with increasing doses of 500 keV C ions, or annealed. The vibration wave numbers in pristine PCS or AHPCS are ~ 2950 and 2900 cm^{-1} (C–H stretching in $Si–CH_3$), 2100 cm^{-1} (Si–H stretching), 1400 cm^{-1} (CH_2 deformation in $Si–CH_3$), $\sim 1355\,cm^{-1}$ (stretching of $Si–CH_2–Si$), $\sim 1260\,cm^{-1}$ ($Si–CH_3$ deformation), 1020 cm^{-1} (CH_2 wagging of $Si–CH_2–Si$), 820 cm^{-1} ($Si–CH_3$ rocking) and 780 cm^{-1} (Si–C stretching) [14]. The last mode is only observed in spectra of annealed specimens, shifted to 800 cm^{-1}, or of heavily irradiated ones. In the case of polysiloxanes, peaks relative to the $Si–CH_3$ bond are shifted to 1270, 1120, 860 cm^{-1}. $Si–CH_2–Si$ modes are, of course, missing and replaced by Si–O–Si stretching modes at ~ 1050 and 805 cm^{-1} (as against 1078 cm^{-1} and 817 cm^{-1} in silica). The latter overlaps with the $Si–CH_3$ rocking mode in spectra of SR350 and SR355, and peaks of C_6H_5 stretching at 1595, 1431 cm^{-1} and of $Si–C_6H_5$ bending at 1134 cm^{-1} appear in spectra of SR355 and PTES. When annealed, the Si–O–Si peak shifts to 1090 cm^{-1}, and the new Si–C one is, in the case of SiOC films, centred at $\sim 790\,cm^{-1}$.

While the Si–OH stretching mode at $\sim 890\,cm^{-1}$ is faint in spectra of pristine polymers because of their good condensation, its intensity increases with irradiation up to doses of 5×10^{13} Au, 5×10^{14} C, 5×10^{15} He as with new peaks characteristic of absorbed water at 3400 and 1630 cm^{-1}. These maximum doses are in agreement with results of ion-beam analysis. The water-related bands vanish for slightly higher fluences, at the same time as other peaks of organic functionalities. All the bands show a progressive smearing out, and are replaced by broad bands of conjugated bonds when the deposited energy reaches values of ~ 40 eV (1×10^{14} Au, 1×10^{15} C). Similar behaviour and

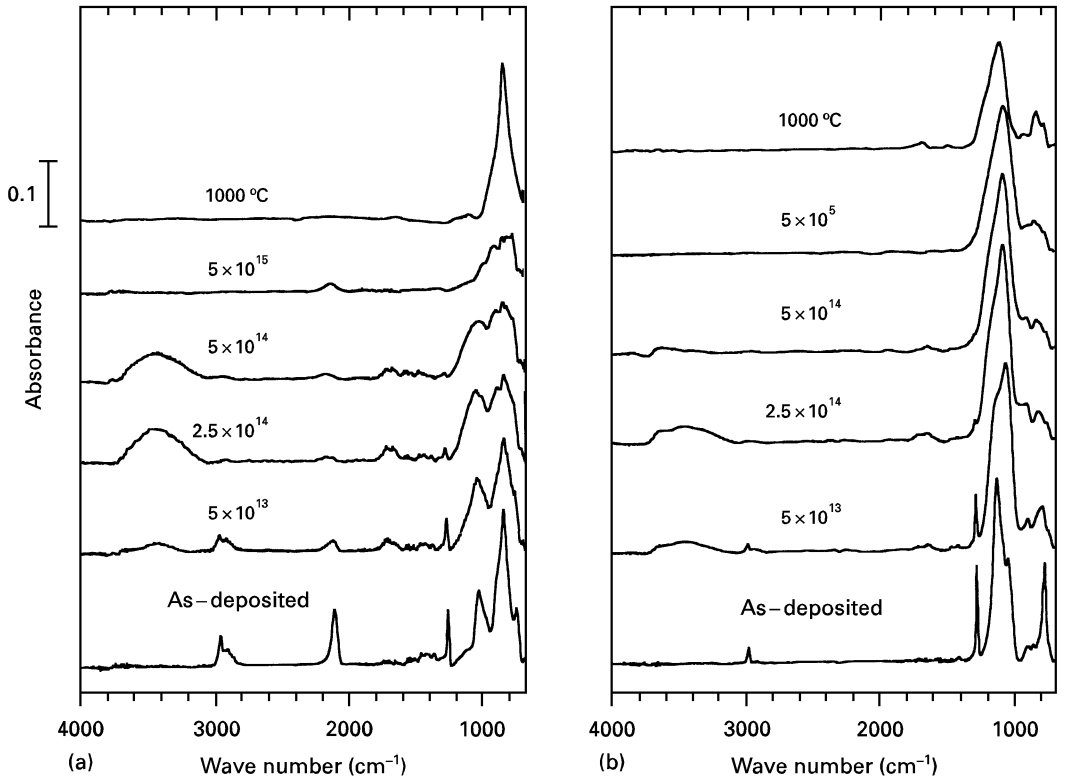

Figure 8 FT–IR spectra of (a) PCS films and (b) SR350 films, irradiated with different doses of carbon ions or annealed.

threshold of collapse into a three-dimensional network are generally found for organic polymers [11]. Note that a small peak located at 2100 cm^{-1} remains visible in the spectra of heavily irradiated specimens of both polycarbosilanes, indicating the retention of some Si–H bonds (however, the absorption coefficient for the Si–H stretching vibration is high, and thus this weak band actually corresponds to a small amount of Si–H). The same band is observed in spectra of the irradiated polysiloxane SR355 for ion fluences higher than that at which water-related bands disappear. Its presence was also reported for some sol–gel derived SiOC glasses after conventional annealing [23].

With respect to spectra of annealed films, the bands of conjugated bonds are significantly broader and shifted toward lower wave numbers (of $\sim 20\ cm^{-1}$ for the main Si–C and Si–O–Si modes) in spectra of films converted by irradiation. An oxygen understoichiometry in silica films [24] or a compressive state of stress [25] can induce such a shift. In the present case, they are more probably due to an higher degree of bond distorsions because of the combination of free radicals at random, and to some atomic disorder in gold-irradiated films. The Si–C peak is narrower in spectra of annealed or irradiated PCS than in those of AHPCS, possibly because of an higher proportion of silicon atoms surrounded by four carbon atoms as stochiometric SiC. This Si–C peak is also more intense and narrower in spectra of annealed PTES than in those of other polysiloxanes.

Raman spectroscopy provided useful information about the chemical bonds of carbon atoms. Indeed, one or two broad bands in the region 1300–1600 cm^{-1} appear in spectra of all irradiated or annealed films while there is none in spectra of pristine films. This result is characteristic of a carbon segregation into clusters. The spectrum of microcrystalline graphite exhibits two bands, referred to as D and G, at well-defined energies of 1355 and 1580 cm^{-1}, the latter shifting up to 1620 cm^{-1} in nanocrystalline or turbostratic graphite, while both bands shift towards each other in amorphous carbon. The higher the degree of sp^3 hybridization, the stronger is this shift until forming a single feature centred at $\sim$1520–1540 cm^{-1} in the most diamond-like films. In the present case, clusters formed in all irradiated films (including AHPCS, despite its stoichiometry being identical to that of the carbide) are found to be diamond-like, while turbostratic graphite precipitates during annealing (Fig. 9). When compared to spectra of very diamond-like carbon films synthetized by ion implantation at low energies (500 eV to 5 keV) or plasma-laser deposition, the peak of irradiated films is broader (full-width at half-maximum $\sim 170\ cm^{-1}$ as against 100 cm^{-1}) and slightly shifted either towards lower frequencies (1510 cm^{-1} for SR350 derived clusters, 1475 for PCS) or towards higher frequencies (1550–1560 cm^{-1} for SR355, PTES). Note that amorphous Si–C also gives rise to less intense modes at 300–600 cm^{-1} (related to Si–Si) and at 700–1000 cm^{-1} (Si–C). However, a broad band at 760 cm^{-1}, comparable to that observed by other authors in spectra of PCS fibres annealed at 1000 °C [22], was observed only in spectra of irradiated PCS but not in our spectra of annealed PCS, most probably because of the different annealing conditions. The two lines of β-SiC at 789 and 967 cm^{-1} appear clearly in spectra of PCS at 1100 °C and they become sharp above 1400 °C, as also do the two C–C bands of graphite [22].

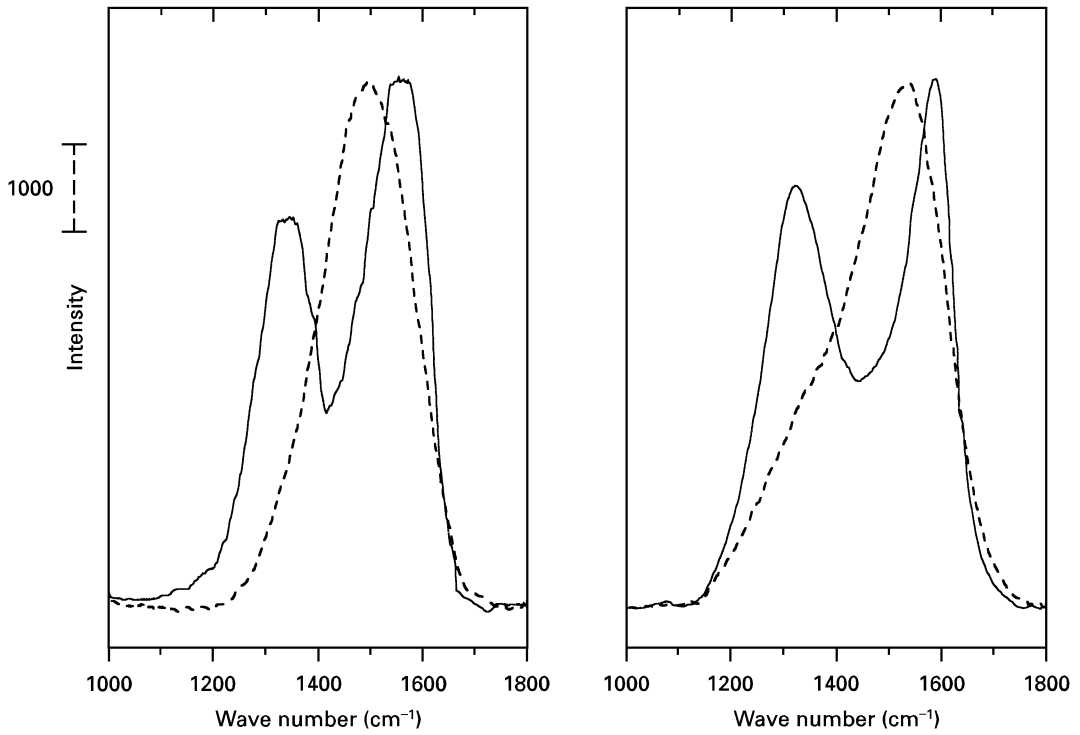

Figure 9 Raman spectra of (a) SR350 films and (b) PTES films: (——) annealed, (– – – –) irradiated 1×10^{16} C.

4. Discussion

4.1. Conversion mechanism

The mechanisms of polmer to ceramic conversion (regardless of their organic or inorganic nature) by ion irradiation are definitely different from the merely chemical decomposition occurring during heat treatments. It has been shown that the conversion kinetics of organic polymers depends critically on the density $S_e + S_n$ of energy deposition, but that the ultimate state is not affected by the proportion of displacements: the amorphous network formed at high doses exhibits diamond-like structure and properties. On the contrary, the thermal cross-linking of bonds with a well-defined sequence (for instance, the intra-chain cyclization of nitriles into pyrido rings followed by the cross-linking of adjacent chains in the case of polyacrilonitrile [26] often leads to the formation of six-membered rings perfectly organized in planes, like in graphite.

The difference between the structural changes promoted by irradiation and heat treatments is still stronger in silicon-based polymers. The pyrolytic conversion into thermodynamically stable compounds, namely SiC, turbostratic graphite and silica, requires long-range rearrangements which are possible only at very high temperatures. These redistribution reactions without changes in the composition [27], compete with other reactions, such as the oxidation of polycarbosilanes leading to the formation of insulating layers around $SiCH_x$ islands, and the evolution of various stable organic molecules with sequences and rates depending on the heat cycle and atmosphere (gas nature and pressure). On the contrary, the high amount of energy transferred locally to electronic shells during ion irradiation promotes an out of equilibrium chemistry, characterized by the formation of many free radicals in a fraction of picosecond and their combination at random (like in a very localized thermal spike). The radiolytic evolution of one or two hydrogen bonds to methyl groups occurs as well as that of a hydrogen bond to silicon in polycarbosilanes, permitting the formation of new $Si–CH_x–Si$ directly, while the latter results selectively from the breaking of the Si–H bonds and the rearrangement of silylene radicals in annealed polycarbosilanes [15]. Even if Si–C and single C–H bonds are particularly stable, they can also be broken at any stage of the conversion, and no parallel reaction competes with the building of the most stable configuration at short range (~ 3 atomic distances): a tetrahedral network of silicon surrounded by four carbons, and of carbon surrounded by either silicon or carbon atoms in excess. Similarly, in polysiloxanes, the most stable amorphous network at short range is built preferentially to the evolution of silanes, then methane and CO, SiO with increasing temperature [16, 17].

Rearrangements during successive cascades lead to the formation of carbon clusters in both types of amorphous networks. Raman spectra indicate that a small part of the carbon atoms of phenyl groups tend to retain their sp^2 hybridization state in clusters of amorphous carbon formed on the spot. On the contrary, carbon atoms of methyl groups diffusing in the amorphous SiOC matrix for piling at random on carbon nuclei, form more diamond-like clusters. It is known that random networks of semiconductors are generally sp^3 hybridized until their size reaches a critical value, and that sp^2 carbon atoms (or silicon, germanium unpaired atoms) segregates as buckles of defects at the periphery of more randomly packed regions [28].

4.2. Conversion kinetics

The fact that the slope of the kinetics of hydrogen evolution (Fig. 4) is independent of the nature and concentration of organic groups in polysiloxanes confirms that C–H bonds in methyl groups are broken as easily as those in phenyl groups upon ionization events. Generally, ΔH values are also very close, except in the case of helium irradiation, and the residual hydrogen contents are roughly in proportion to those of carbon (Tables II and III): of the order of 0.30 hydrogen per carbon. One can reasonably conclude that similar proportions of hydrogen remain bound to carbon atoms in clusters derived directly from phenyl groups or in clusters and isolated carbon atoms derived from methyl ones. The initial yield of hydrogen evolution is faster in polycarbosilanes than in polysiloxanes, but the rate of increase at higher fluences of carbon, gold irradiation is very similar, as is also the residual H/C content ratio. On the other hand, the slower kinetics in helium irradiated films and their oxidizability must be ascribed to a smaller density of defects produced in individual ion cascades. As in the case of organic polymers, free radicals formed by ionization have a smaller probability to combine into more stable cross-links than those formed in dense cascades. Silicon atoms bonded to the phenyl groups appear a little more sensitive to this oxidation. One can note that even if 1 OH/Si must be included in the balance of groups sensitive to ionization in the case of PTES films, the relative yields of hydrogen release are, however, very comparable.

The logarithmic law of compaction and hydrogen loss presently observed is not correlated with a theoretical model. Calcagno and Foti [29] used a classical model of radiation-induced transformation with a constant cross-section $\sigma \times S_e$, implying that the rate of decrease of the volume fraction C of the original polymer is given by the differential equation: $dC/d\Phi = C \times \sigma \times S_e$. With this crude hypothesis, they established that the thickness, t, would tend towards an ultimate value, t_f, and the hydrogen concentration, z, towards z_f according to the following equations

$$(t_0 - t) = (t_0 - t_f)(1 - e^{-\sigma_t S_e \Phi}) \quad (1)$$

$$\left(\frac{1}{z} - \frac{1}{z_f}\right) = \left(\frac{1}{z_0} - \frac{1}{z_f}\right) e^{-\sigma_H S_e \Phi}) \quad (2)$$

Note that a logarithmic law has the same simple meaning of a decreasing probability of transformation as the concentration of groups able to transform decreases. Actual variations of t and z in the presently studied polymers are not well fitted with the above formula (approximate values of σ_t and σ_H are of the order of 0.02 atom eV^{-1}). A more realistic model would take into account the dependency of the ionization efficiency, σ, on the mass of ions, which was observed here and also in the case of organic polymers [11]. In other terms, a better differential equation would be of the type $dC/d\Phi = C \times \sigma \times S_e^n$ with a power n higher than 1. Nevertheless, further developments are illusory, because the mechanism of transformation involves several parallel processes with different cross-sections. Indeed, variations of the ionization efficiency, σ, in C–H_x moities with an increasing bond strength as x decreases and in newly formed clusters, are disregarded in such formulations. The influence of the atomic disordering by means of nuclear collisions on both the cross-section and the saturation levels, t_f and z_f, are not considered.

The reasons for the compaction in the ratio of the hydrogen H loss or of its square, according to the type of polymer, are probably also too complex for proposing a straightforward explanation. Crudely speaking, the quadratic law observed in the case of PCS may be ascribed to the fact that, in its original structure, there are two CH_2 groups on neighbouring sites which can combine to release directly one hydrogen molecule when one of the bonds is broken during a single ionization event.

5. Conclusion

Ion irradiation of preceramic polymers films allow amorphous ceramic coatings to be obtained. The systematic investigation of the conversion kinetics, which was performed as a function of the ion dose and mass, has shown that it is controlled by two key parameters: the linear density of energy transferred to electron shells, and the ratio of this energy density to that used to displace atoms. The combination of radicals formed during a single cascade accelerates the conversion kinetics (in PCS) and helps to avoid their reaction with the atmosphere at the issue of the irradiation.

Raman analyses of the presently studied polysiloxanes indicate that small side groups, like methyls, tend to segregate in clusters with a more diamond-like character than those formed on the spot by irradiation of larger groups (like phenyl rings). Probably the cyclic or aliphatic nature of groups for a given carbon atom number is also of importance. This effect was not observed in our investigations on organic polymers in which no segregation could occur.

Further evidence of the effect of atomic displacements on the structural order at high ion fluences and of the more or less diamond-like nature of formed clusters according to their origin, is given by the mechanical strength of films and their thermochemical stability, as discussed in Part II [13].

Acknowledgements

Thanks are due to J. Salomon, Laboratoire des Musées de France, Louvres, Paris, and to G. Sagon, LASIR CNRS Center, Thiais, near Paris, for their help in NRA and Raman analyses. The authors are also grateful to W. Sherwood, Starfire Systems Inc. (Watervliet, NY) for kindly donating the AHPCS preceramic polymer used in the experiments.

References

1. C. J. BRINKER and G. W. SCHERER, "Sol-Gel Science: the physics and chemistry of sol-gel processing" (Academic Press, Boston, MA, 1990) p. 787.
2. C. -J. CHU, G. D. SORARÙ, F. BABONNEAU and J. D. MACKENZIE, in "Amorphous and Crystalline Silicon

Carbide and related Materials II", Springer Proceedings in Physics, Vol. 43, edited by M. M. Rahman and G. L. Harris (Springer, Heidelberg, 1989) p. 66.
3. M. HARRIS, T. M. CHAUDHARY, L. DRZAL and R. M. LAINE, *Mater. Sci. Eng.* **A195** (1995) 223.
4. T. M. CHAUDHARY, H. HO, L. DRZAL, M. HARRIS and R. M. LAINE, *ibid.* **A195** (1995) 237.
5. V. Z. -H. CHAN, J. B. ROTHMAN, P. PALLADINO, L. G. SNEDDON and R. J. COMPOSTO, *J. Mater. Res.* **11** (1996) 373.
6. P. COLOMBO, T. E. PAULSON and C. G. PANTANO, *J. Sol-Gel. Sci. Technol.* **2** (1994) 601.
7. M. R. MUCALO, N. B. MILESTONE, I. C. VICKRIDGE and M. V. SWAIN, *J. Mater. Sci.* **29** (1994) 4487.
8. M. R. MUCALO and N. B. MILESTONE, *ibid.* **29** (1994) 5934.
9. J. C. PIVIN, P. COLOMBO and M. TONIDANDEL, *J. Am. Ceram. Soc.* **79** (1996) 1967.
10. J. C. PIVIN and P. COLOMBO, *Nucl. Instrum. Methods* **B120** (1996) 262.
11. J. C. PIVIN, P. VEIL, G. ZALCZER and G. MARLETTA, *ibid.* **B105** (1995) 192.
12. P. T. VENKATESAN, *ibid.* **B7** (1985) 461.
13. J. C. PIVIN, and P. COLOMBO *J. Mater. Sci.* **32** (1997) in press.
14. P. S. YAJIMA, in "Handbook of Composites", Vol. 1, "Strong Fibers", edited by W. Watt and B. V. Perov (Elsevier Science, New York, NY, 1985) p. 202.
15. L. V. INTERRANTE, C. W. WHITMARSH, W. SHERWOOD, H.-J. WU, R. LEWIS and G. MACIEL, *Mater. Res. Soc. Symp. Proc.* **346** (1994) 593.
16. G. M. RENLUND, S. PROCHAZA and R. H. DOREMUS, *J. Mater. Res.* **6** (1991) 2716.
17. *Idem*, *ibid.* **6** (1991) 2723.
18. E. COTTEREAU, J. CAMPLAN, J. CHAUMONT, R. MEUNIER and H. BERNAS, *Nucl. Instrum. Methods* **B45** (1990) 293.
19. J. C. PIVIN, G. BRUSATIN, G. ZALCZER, *Thin Solid Films* **287** (1996) 65.
20. J. P. BIERSACK, *Nucl. Instrum. Methods* **B17** (1980) 257.
21. *Idem*, *ibid.* **B27** (1987) 21.
22. E. BOUILLON, F. LANGLAIS, R. PAILLER, R. NASLAIN, F. CRUEGE, P. V. HUONG, J. C. SARTHOU, A. DELPUECH, C. LAFFON, P. LAGARDE, M. MONTHIOUX and A. OBERLIN, *J. Mater. Sci.* **26** (1991) 1333.
23. L. BOIS, J. MAQUET, F. BABONNEAU, H. MUTIN and D. BAHLOUL, *Chem. Mater.* **6** (1994) 796.
24. M. SENDOVA-VASSILEVA, N. TZENOV, D. DIMOVA-MALINOVSKA, K. V. JOSEPOVITS, *Mater. Res. Soc. Symp. Proc.* **417** (1996) 395.
25. J. T. FITCH, C. H. BJORKMAN, J. J. SUMAKERIS, G. LUCOVSKY, *ibid.* **130** (1989) 289.
26. F. HOUZE, L. BOYER, S. NOEL, P. VIEL, G. LECAYON and J. M. BOULIN, *Synth. Metals* **62** (1994) 207.
27. V. BELOT, J. P. CORRIU, D. LECLERC, P. H. MUTIN, A. VIOUX, *J. Polym. Sci. A Polym. Chem.* **30** (1992) 613.
28. J. ROBERTSON, *Adv. Phys.* **35** (1986) 317.
29. L. CALCAGNO and G. FOTI, *Nucl. Instrum. Methods* **B19/20** (1987) 895.

Received 25 March
and accepted 29 May 1997